

2 Theory of Elementary Particles

M. Baker, M. Bordone, F. Buccioni, L. Buonocore, D. Buttazzo, X. Chen, L. Cieri, C. Cornella, S. Devoto, J. Fuentes-Martin, T. Gehrmann, M. Grazzini, N. Greiner, A. Greljio, M. Höfer, D. Hulme, A. Ilnicka, T. Jezo, D. Kara, A. Karlberg, M. König, G. Isidori, J.N. Lang, J. Mazzitelli, J. Mo, D. Müller, J. Niehues, A. Patteri, S. Pozzorini, A. Primo, H. Sargsyan, A. Signer, M. Schönherr, S. Trifinopoulos, Y. Ulrich, D. van Dyk, J.Y. Yook, H. Zhang, M. Zoller

in collaboration with:

University of Belo Horizonte, CERN, IMSc Chennai, University of Coimbra, TU Dresden, Durham University, University of Edinburgh, INFN and University of Firenze, Freiburg University, University of Granada, Lisbon University, University of Lyon, Stephan Insistue Ljubljana, Mainz University, Michigan State University, University of Milano Bicocca, INFN and University of Milano, MPI Munich, INFN and University of Napoli, Scuola Normale Pisa, INFN and University of Padova, Peking University, University of San Martin, IFIC Valencia, ETH Zürich.

The particle theory group at the Physik-Institut works on a broad spectrum of research projects related to the interpretation of data from high energy particle colliders. These cover precision calculations of benchmark observables, simulation of full collider events, identification of optimal observables for searches and measurements, physics beyond the Standard Model, as well as developments of calculational techniques. We summarize some highlights of last year's research below.

2.1 Theoretical predictions for dark-matter searches at the LHC

The signature of missing transverse energy (MET) recoiling against high-energy jets is one of the most powerful tools in the interpretation of data from hadron colliders. In the Standard Model (SM), MET+jet final states arise from the production of jets in association with electroweak bosons that decay into neutrinos in the processes $pp \rightarrow Z(\rightarrow \nu\bar{\nu}) + \text{jet}$ and $pp \rightarrow W^\pm(\rightarrow \ell\nu) + \text{jet}$. But MET+jet production is also an almost omnipresent feature of theories of physics beyond the SM (BSM). In particular, MET+jet events are the most powerful probes of dark matter at the LHC. The sensitivity of such searches depends in a critical way on the precision at which the SM background processes $pp \rightarrow V + \text{jet}$ with $V = W^\pm, Z$ can be controlled. In practice, systematic uncertainties are minimised by performing accurate measurements of $V + \text{jet}$ processes in control regions dominated by visible signatures, i.e. $\gamma + \text{jet}$, $Z(\rightarrow \ell^+\ell^-) + \text{jet}$ or $W(\rightarrow \ell\nu) + \text{jet}$ production with a visible lepton, and extrapolating such measurements to the case of invisible $V + \text{jet}$ signatures in the region of high transverse-momentum (p_T), where

a dark-matter signal may show up. Such extrapolations are based on theoretical predictions. In particular, they require a precise theoretical understanding of the correlation between different $V + \text{jet}$ processes and different p_T regions.

In this context, recent advances in perturbative calculations, driven by research at our institute [1–4], have opened the door to significant sensitivity improvements in dark matter searches. A combination of state-of-the-art calculations for all relevant $V + \text{jet}$ processes was presented in Ref. [5]. Besides including QCD and electroweak (EW) quantum corrections at the highest available order, this study provides the first systematic methodological framework for the application of high-precision theory predictions to MET+jet searches. In particular, we have introduced and applied various new approaches to estimate uncertainties and their correlations across different processes and p_T regions.

The long-standing problem of how to treat the correlation of higher-order effects across different $V + \text{jet}$ processes is addressed by a quantitative method that permits to split QCD effects into universal and process-dependent parts. Amongst others, this is achieved by using a dynamic definition of photons in the high-energy regime. Specifically, we have shown that isolating photons from the surrounding collinear QCD radiation by means of a dynamic cone it is possible to maximise the level of QCD correlation between $\gamma + \text{jet}$ and $W/Z + \text{jet}$ production, thereby minimising the uncertainties in the extrapolation from $\gamma + \text{jet}$ production to dark-matter backgrounds.

Given the strong impact of EW corrections on the shapes of p_T distribution for the various $V + \text{jet}$ processes and process ratios, NLO EW corrections have been sup-

plemented by the dominant Sudakov EW logarithms at NNLO [6, 7]. Moreover, in order to assess unknown higher-order effects stemming from the interplay of large QCD and EW corrections, we have introduced a dedicated method that allows one to exploit NLO EW calculations for $V + 2\text{jet}$ production [2] in order to quantify $\mathcal{O}(\alpha_s)$ corrections in terms of a simple factorised Ansatz plus extra non-factorising terms. Finally, also the uncertainties associated with parton distribution functions (PDFs) have been assessed in detail.

In Fig. 2.1 we present predictions and uncertainty esti-

mates for the different $V+\text{jet}$ processes and process ratios. All sources of QCD and EW uncertainties are combined in quadrature overlaying the remaining PDF uncertainties as a result of the N(N)LO QCD and nNLO EW corrections, the level of theoretical predictions in the p_T distributions for individual $V+\text{jet}$ processes reaches the 5–10% level up to about 1 TeV and the 10–20% level up to about 2 TeV. In the process ratios theoretical uncertainties cancel to a large extent. In particular, in the Z/W ratio remaining uncertainties are at the level of only 1–2% up to 1 TeV

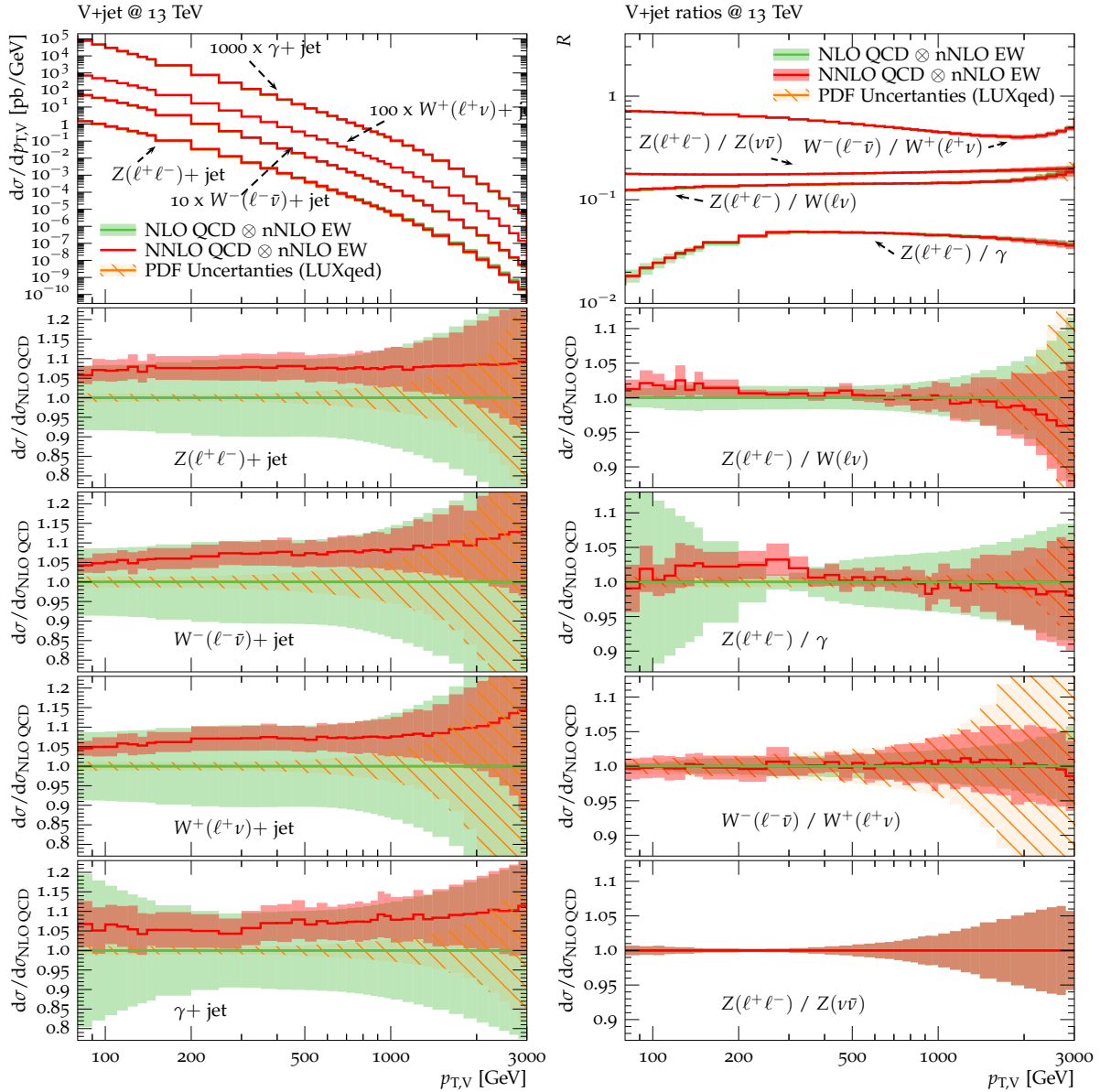


FIG. 2.1 – Theoretical predictions for $V+\text{jet}$ spectra (left) and ratios (right) at 13 TeV including (N)NLO QCD and nNLO EW corrections. The lower frames show the relative impact of corrections and theory uncertainties. The green and red bands correspond to the combination of perturbative uncertainties, while PDF uncertainties are shown as hashed orange bands. See Ref. [5] for details.

and below 5% up to 2 TeV. Similarly, the Z/γ ratio is constrained at the 5% level up to 2 TeV. Noteworthy, including the NNLO QCD corrections the process ratios remain very stable and in particular within the uncertainty estimates based on NLO QCD. This reflects the fact that QCD uncertainties are very well under control: taking at face value the NNLO QCD systematics we are at the level of few percent all the way up to the multi-TeV scale, and at large p_T we are dominated by EW and PDF uncertainties. The latter are below the perturbative uncertainties in all nominal distributions and all but the W^-/W^+ ratio, where a precise measurement at high p_T could help to improve PDF fits.

Overall, it is possible to obtain precise theoretical control both for vector-boson p_T distributions, and their ratios, at the level of a few percent over a wide range of p_T . These results and the proposed methodology have already been adopted in experimental analyses by ATLAS and CMS, leading to substantial improvements in the sensitivity of dark-matter searches. The benefits of high-precision theoretical calculations are going to be further enhanced once high-luminosity LHC data become available.

- [1] S. Kallweit, J. M. Lindert, P. Maierhofer, S. Pozzorini, and M. Schoenherr, *NLO electroweak automation and precise predictions for W +multijet production at the LHC*, JHEP **04** (2015) 012, [arXiv:1412.5157].
- [2] S. Kallweit, J. M. Lindert, P. Maierhofer, S. Pozzorini, and M. Schönherr, *NLO QCD+EW predictions for V + jets including off-shell vector-boson decays and multijet merging*, JHEP **04** (2016) 021, [arXiv:1511.0869].
- [3] A. Gehrmann-De Ridder, T. Gehrmann, E. W. N. Glover, A. Huss, and T. A. Morgan, *Precise QCD predictions for the production of a Z boson in association with a hadronic jet*, Phys. Rev. Lett. **117** (2016), no. 2 022001, [arXiv:1507.0285].
- [4] A. Gehrmann-De Ridder, T. Gehrmann, E. W. N. Glover, A. Huss, and T. A. Morgan, *The NNLO QCD corrections to Z boson production at large transverse momentum*, JHEP **07** (2016) 133, [arXiv:1605.0429].
- [5] J. M. Lindert *et al.*, *Precise predictions for V + jets dark matter backgrounds*, Eur. Phys. J. **C77** (2017), no. 12 829, [arXiv:1705.0466].
- [6] J. H. Kuehn, A. Kulesza, S. Pozzorini, and M. Schulze, *One-loop weak corrections to hadronic production of Z bosons at large transverse momenta*, Nucl. Phys. **B727** (2005) 368-394, [hep-ph/0507178].
- [7] J. H. Kuehn, A. Kulesza, S. Pozzorini, and M. Schulze, *Electroweak corrections to hadronic production of W bosons at large transverse momenta*, Nucl. Phys. **B797** (2008) 27-77, [arXiv:0708.0476].

2.2 Higgs boson pair production at NNLO

One of the primary goals of the LHC programme in the next decades is the detailed study of Higgs boson properties. In particular, the high-luminosity upgrade of the LHC is expected to provide direct constraints on the Higgs boson trilinear coupling from Higgs boson pair production, which may reveal whether the Higgs potential is indeed Standard-Model like. A detailed theoretical understanding of the Higgs boson pair production processes is thus mandatory. The most important production channel of a pair of Higgs bosons at the LHC is $gg \rightarrow hh$, which proceeds through triangular and box diagrams, where the dominant contribution is given by the top quark. Unfortunately, only the triangles are sensitive to the Higgs trilinear coupling, and cancellations among the diagrams, together with the small available phase space, make the cross section extremely small.

The $gg \rightarrow hh$ cross section at leading order (LO) is known since quite some time. The next-to-leading-order (NLO) corrections with full top quark mass (M_t) dependence, involving two-loop diagrams with several mass scales, became available only recently [8,9]. Alternatively, to compute yet higher-order perturbative contributions, it is possible to use a Higgs Effective Field Theory approach (HEFT), in which the top quark is integrated out.

In Ref. [10] we have presented a new calculation of the double Higgs cross section at next-to-next-to-leading order (NNLO) in QCD perturbation theory. Our calculation is based on the publicly available computational framework MATRIX [11], which allows the user to perform fully differential NNLO calculations for a wide class of processes at hadron colliders. We start from the exact two-loop amplitude, which is implemented in a dedicated version of MATRIX, and we can thus reproduce the NLO result of Ref. [8,9]. In our reference calculation, denoted by $\text{FT}_{\text{approx}}$, the NNLO contributions are evaluated by using the exact one-loop amplitude for double real emission combined with the real-virtual and double-virtual contributions in the HEFT, but reweighted with the exact Born amplitudes. More precisely, each NNLO contribution is rescaled with the factor

$$\mathcal{R}(ij \rightarrow HH + X) = \frac{\mathcal{A}_{\text{Full}}^{\text{Born}}(ij \rightarrow HH + X)}{\mathcal{A}_{\text{HEFT}}^{(0)}(ij \rightarrow HH + X)}. \quad (2.1)$$

This approximation, which includes the most advanced perturbative information available at present for this process, is denoted by $\text{NNLO}_{\text{FTapprox}}$, and is supposed to provide the best perturbative prediction. Another approximation, denoted by $\text{NNLO}_{\text{NLO-i}}$, can be obtained

\sqrt{s}	13 TeV	14 TeV	27 TeV	100 TeV
NLO [fb]	27.78 ^{+13.8%} _{-12.8%}	32.88 ^{+13.5%} _{-12.5%}	127.7 ^{+11.5%} _{-10.4%}	1147 ^{+10.7%} _{-9.9%}
NLO _{FTapprox} [fb]	28.91 ^{+15.0%} _{-13.4%}	34.25 ^{+14.7%} _{-13.2%}	134.1 ^{+12.7%} _{-11.1%}	1220 ^{+11.9%} _{-10.6%}
NNLO _{NLO-i} [fb]	32.69 ^{+5.3%} _{-7.7%}	38.66 ^{+5.3%} _{-7.7%}	149.3 ^{+4.8%} _{-6.7%}	1337 ^{+4.1%} _{-5.4%}
NNLO _{FTapprox} [fb]	31.05 ^{+2.2%} _{-5.0%}	36.69 ^{+2.1%} _{-4.9%}	139.9 ^{+1.3%} _{-3.9%}	1224 ^{+0.9%} _{-3.2%}
M_t unc. NNLO _{FTapprox}	±2.6%	±2.7%	±3.4%	±4.6%
NNLO _{FTapprox} /NLO	1.118	1.116	1.096	1.067

TAB. 2.1 – Inclusive cross sections for Higgs boson pair production for different centre-of-mass energies at NLO and NNLO within the considered approximations. Scale uncertainties are reported as superscript/subscript. The estimated top quark mass uncertainty of the NNLO_{FTapprox} predictions is also presented. The numerical uncertainties are estimated to be at the per mille level.

by reweighting the exact NLO result for the invariant mass distribution of the Higgs boson pair with the NNLO/NLO ratio obtained in the HEFT. We consider centre-of-mass energies of 13, 14, 27 and 100 TeV. We use the values $M_h = 125$ GeV for the Higgs boson mass and $M_t = 173$ GeV for the pole mass of the top quark. We use the PDF4LHC15 sets of parton distribution functions (PDFs), with parton densities and as evaluated at each corresponding perturbative order (i.e., we use the $(k+1)$ -loop running as at N^k LO, with $k = 1, 2$). As renormalisation and factorisation scales, we use the central value $\mu_0 = M_{hh}/2$, and we obtain scale uncertainties via the usual 7-point scale variation.

The approximated NNLO cross sections computed as discussed above are reported in Table 2.1. The NNLO effect ranges from about +12% at $\sqrt{s} = 13$ TeV to about +7% at $\sqrt{s} = 100$ TeV. For the considered approximations and collider energies the scale uncertainties are significantly reduced when including the $\mathcal{O}(as^4)$ NNLO corrections. This reduction is largest for the NNLO_{FTapprox} approximation. For instance, at 14 TeV the total scale uncertainty is reduced from about ±13% at NLO to +2% – 5% at NNLO_{FTapprox}, i.e. by about a factor of three. This reduction of the scale uncertainties is stronger as we increase the collider energy and at 100 TeV it approaches a factor of five. As is well known, scale uncertainties can only provide a lower limit on the true perturbative uncertainties. In particular, from Table 2.1 we see that the difference between the NNLO and NLO central predictions is always larger than the NNLO scale uncertainties (although within the NLO uncertainty bands). In any case, the strong reduction of scale uncertainties, together with the moderate impact of NNLO corrections, suggests a significant improvement in the perturbative convergence as we move from NLO to NNLO.

While our calculation includes the exact dependence on the top quark mass up to NLO, at NNLO the top mass effects are included in an approximate way. The NNLO_{FTapprox} result represents our best prediction, and for a conservative estimate of the uncertainty of this approximation we compare it against our “next-to-best” prediction. Our estimate for the finite top quark mass uncertainty of our NNLO_{FTapprox} result is defined as *half the difference between the NNLO_{FTapprox} and the NNLO_{NLO-i} approximations*, and is reported in Table 2.1 for the different values of \sqrt{s} . At $\sqrt{s} = 14$ TeV the uncertainty is ±2.7%, whereas at $\sqrt{s} = 100$ TeV it increases to ±4.6%. A more detailed discussion on this uncertainty and additional results can be found in Ref. [10].

- [8] S. Borowka, N. Greiner, G. Heinrich, S. Jones, M. Kerner, J. Schlenk, U. Schubert, and T. Zirke, *Higgs Boson Pair Production in Gluon Fusion at Next-to-Leading Order with Full Top-Quark Mass Dependence*, Phys. Rev. Lett. **117** (2016), no. 1 012001, [arXiv:1604.0644]. [Erratum: Phys. Rev. Lett. **117**,no.7,079901(2016)].
- [9] S. Borowka, N. Greiner, G. Heinrich, S. P. Jones, M. Kerner, J. Schlenk, and T. Zirke, *Full top quark mass dependence in Higgs boson pair production at NLO*, JHEP **10** (2016) 107, [arXiv:1608.0479].
- [10] M. Grazzini, G. Heinrich, S. Jones, S. Kallweit, M. Kerner, J. M. Lindert, and J. Mazitelli, *Higgs boson pair production at NNLO with top quark mass effects*, arXiv:1803.0246.
- [11] M. Grazzini, S. Kallweit, and M. Wiesemann, *Fully differential NNLO computations with MATRIX*, arXiv:1711.0663.

2.3 Precise predictions for transverse momentum distributions of electroweak bosons

The production of electroweak (EW) gauge bosons with subsequent leptonic decay, known as the Drell–Yan process, is one of the most prominent processes at hadron–hadron colliders such as the LHC. Not only are the gauge bosons produced in abundance, but the clean leptonic signature allows this class of processes to be measured with great precision. As a consequence, the Drell–Yan-like production of W and Z bosons is among the most important ‘standard candles’ at hadron colliders and, as such, has a wide range of applications.

The transverse-momentum spectrum of the gauge bosons (p_T^V) takes a particularly important role in this respect: Different kinematical regimes of this observable probe various aspects of the predictions, such as resummation and non-perturbative effects at low p_T^V , fixed-order predictions at intermediate to high p_T^V , and also electroweak Sudakov logarithms at very high p_T^V . As such, detailed theory–data comparisons of this observable constitute crucial probes to test the Standard Model (SM) predictions. We recently computed [12] the $\mathcal{O}(\alpha_s^3)$

NNLO QCD corrections to W production at finite transverse momentum with leptonic decay, which is closely related to the Z transverse momentum distribution discussed in Refs. [13–15].

Figure 2.2 shows the normalised transverse-momentum distribution of the W boson in the electron and muon channels. The NLO corrections are between 10–40% with residual scale uncertainties at the level of around $\pm 10\%$. Although the scale-uncertainty bands at NLO mostly cover the experimental data points, systematic differences in the shape between data and the central theory prediction are visible. In view of the experimental precision, this clearly demonstrates the necessity of higher-order predictions with smaller uncertainties in order to discriminate such behaviours. The NNLO corrections are positive and between 5–10% in the intermediate-to high- p_T^W region. Towards lower p_T^W , the NNLO corrections become smaller and turn negative in the lowest- p_T^W bin. The residual scale uncertainties reduce to the level of about $\pm 2\%$ and overlap with the NLO scale bands, exhibiting good perturbative convergence. Most notably, we observe that the shape distortion induced by the NNLO corrections brings the central predictions in line with the measured distributions.

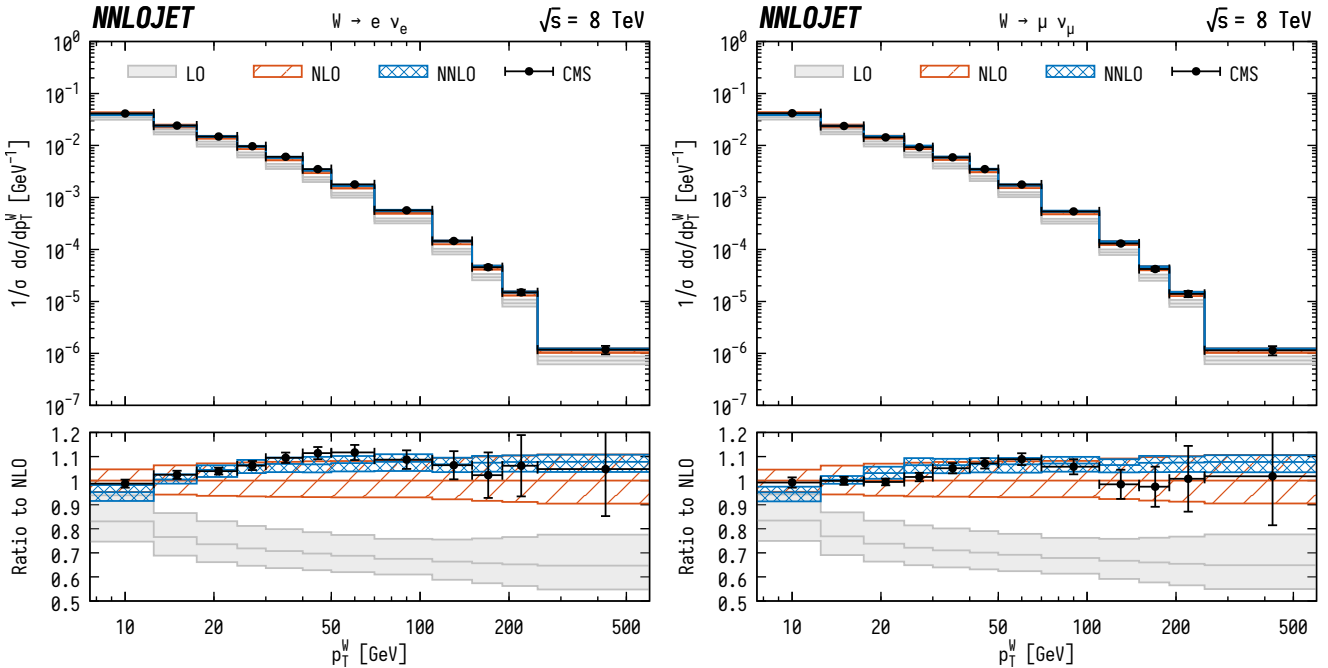


FIG. 2.2 – Normalised p_T^W distribution for $W = W^+ + W^-$ production with subsequent decay into electrons (left) and muons (right). Predictions at LO (gray fill), NLO (orange hatched), and NNLO (blue cross-hatched) are compared to CMS data from Ref. [16]. The bands correspond to scale uncertainties estimated as described in the main text.

Figure 2.3(left) shows the ratio between the normalised distributions of the W boson processes. The ratio is close to one in the lowest p_T^W bin and rises up to ~ 1.1 at $p_T^W \approx 150$ GeV, where it turns over and slowly decreases to 0.9 at $p_T^W = 500$ GeV. The central predictions remain remarkably stable between the different orders, resulting in K -factors that are very close to one. However, the precision of the theory prediction is substantially improved by going to higher orders: While the scale uncertainties at NLO are between ± 10 – 20% , the NNLO corrections reduce the uncertainties to the level of $\pm 5\%$ across most of the p_T^W range, never exceeding $\pm 10\%$.

The ratio between the Z - and W -boson processes are shown in Fig. 2.3(right). Here, the ratio is again close to one in the low- p_T^V bin and shows a steady increase towards higher p_T^V , reaching about 1.5 at $p_T^V \sim 500$ GeV. As was the case for the W^-/W^+ ratio, the QCD corrections are very stable and leave the central predictions largely unaffected, supporting the expected similarity of QCD corrections between Z and W production. The higher-order corrections however have a big impact on the scale uncertainties, which are reduced by more than a factor of two across almost all p_T^V -bins by going from NLO to NNLO and are at the level of ± 5 – 10% .

6

The results presented here pave the way towards stress-testing SM predictions using the precise experi-

mental data that are available for the p_T^V spectra and related observables and to reduce theory uncertainties in the extraction of PDFs and parameters such as M_W .

- [12] A. Gehrmann-De Ridder, T. Gehrmann, E. W. N. Glover, A. Huss, and D. M. Walker, *NNLO QCD corrections to the transverse momentum distribution of weak gauge bosons*, Phys. Rev. Lett. **120** (2018), no. 12 122001, [arXiv:1712.0754].
- [13] A. Gehrmann-De Ridder, T. Gehrmann, E. W. N. Glover, A. Huss, and T. A. Morgan, *The NNLO QCD corrections to Z boson production at large transverse momentum*, JHEP **07** (2016) 133, [arXiv:1605.0429].
- [14] A. Gehrmann-De Ridder, T. Gehrmann, E. W. N. Glover, A. Huss, and T. A. Morgan, *NNLO QCD corrections for Drell-Yan p_T^Z and ϕ observables at the LHC*, JHEP **11** (2016) 094, [arXiv:1610.0184].
- [15] R. Gauld, A. Gehrmann-De Ridder, T. Gehrmann, E. W. N. Glover, and at the LHC, A. Huss, *Precise predictions for the angular coefficients in Z-boson production*, JHEP **11** (2017) 003, [arXiv:1708.0000].
- [16] CMS Collaboration, V. Khachatryan *et al.*, *Measurement of the transverse momentum spectra of weak vector bosons produced in proton-proton collisions at $\sqrt{s} = 8$ TeV*, JHEP **02** (2017) 096, [arXiv:1606.0586].

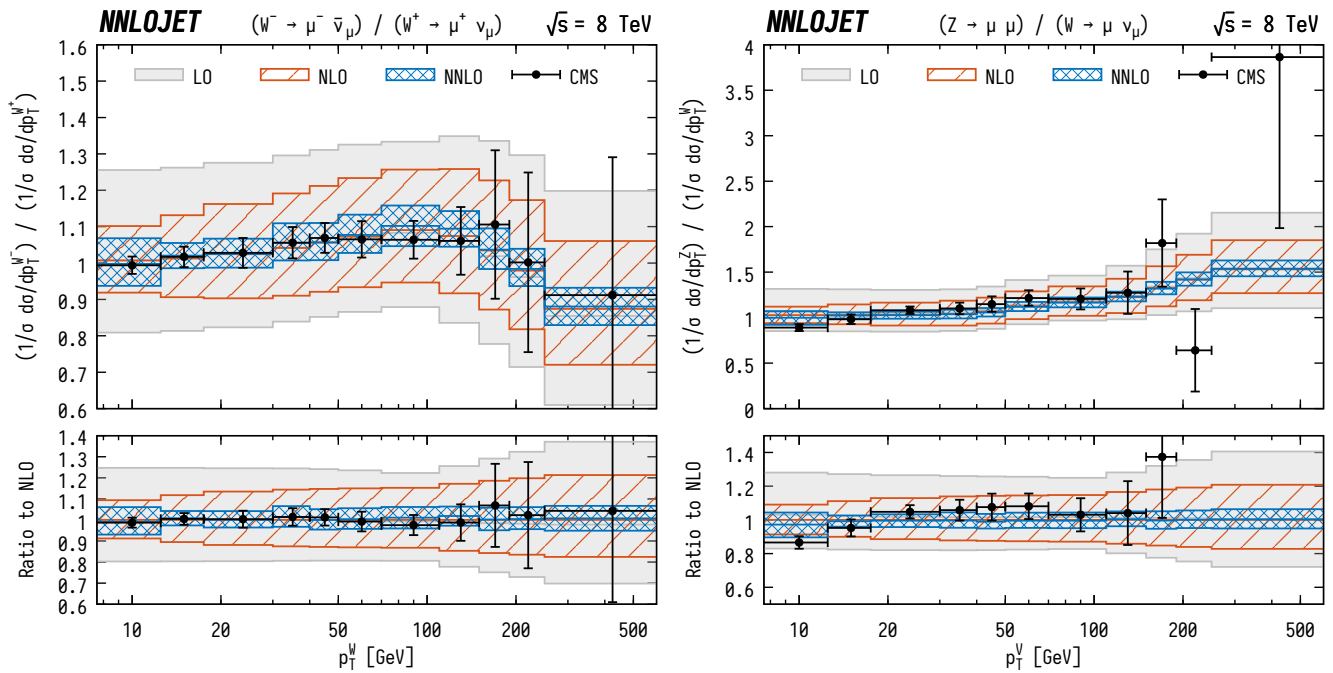


FIG. 2.3 – Ratio of normalised p_T^W distributions between W^- and W^+ production (left) and between Z and $W = W^+ + W^-$ production (right) in the muon channel. Predictions at LO (gray fill), NLO (orange hatched), and NNLO (blue cross-hatched) are compared to CMS data from Ref. [16]. The bands correspond to scale uncertainties estimated as described in the main text.

2.4 Regularization-scheme dependence

Intermediate results in perturbative higher-order calculations in gauge theories such as QED or QCD suffer from divergences. In order to give these expressions a well-defined mathematical meaning, a regularization is needed. For a final physical result, the regularization can be removed and a finite, regularization-scheme independent answer is obtained.

For most calculations, conventional dimensional regularization (CDR) is used, whereby the dimension for all quantities is moved away from the physical value of 4 to $D \equiv 4 - 2\epsilon$. The singularities then manifest themselves as poles in $1/\epsilon$. While this is a very elegant and powerful method there are circumstances where other methods are advantageous.

Broadly speaking there are two classes of schemes. First there are variations of CDR where only some quantities are moved to D dimensions and others are kept in 4 dimensions. Second, there are schemes that work entirely in 4 dimensions and define subtraction terms to regularize the singularities. Some schemes offer various advantages for the computation of particular parts of a full physical result. For example, numerical methods often rely on some quantities being defined in strictly four dimensions. In order to be able to combine separate parts computed with different regularization schemes it is mandatory to precisely understand their relation and how to convert a partial result from one scheme to another.

Our group has worked on a consistent formulation of several schemes and their comparison to others. Following a workshop that took place at the University of Zurich, this has culminated in an article [17] that compares and translates the various schemes. Virtually all international groups working on this topic have participated and new relations between proposed regularization schemes have been discovered.

Among the long-standing problems of CDR is the treatment of γ_5 , an inherently four-dimensional object that cannot be defined consistently in D dimensions. Building on [17], we have revisited this problem and studied how to consistently implement γ_5 in schemes other than CDR [18]. The clarification of such technical questions opens the possibility to develop more efficient computational techniques for theories that involve γ_5 .

[17] C. Gnendiger *et al.*, *To d, or not to d: recent developments and comparisons of regularization schemes*, Eur. Phys. J. C77 (2017), no. 7 471, [arXiv:1705.0182].

[18] C. Gnendiger and A. Signer, γ_5 in FDH, arXiv:1710.0923.

2.5 Flavour physics within and beyond the Standard Model

Continuing the research line started in 2015, also in 2017 we have devoted most of our research efforts on analysing origin and implications of the evidences of Lepton Flavour Universality (LFU) violations observed in B physics. We have analysed this phenomenon both from a pure phenomenological perspective and in the context of motivated extensions of the Standard Model (SM). Our research has been articulated along two main directions.

- *New physics analyses based on Effective Theory approaches and simplified models.*

Completing the work started in 2015, we have presented an extensive analysis (and a complete solution) of the problem of combining the two sets of anomalies, namely i) the breaking of τ - μ universality in $B \rightarrow D^{(*)} \ell \nu$ decays and ii) the breaking of μ - e universality in $B \rightarrow K \ell^+ \ell^-$ decays, within a common Effective Field Theory approach [19]. Using the same approach, we have investigated the possible implication of these anomalies on rare K decays. As we have shown [20], the $K \rightarrow \pi \nu \bar{\nu}$ decays could be particularly interesting probes of LFU breaking dynamics, being the only kaon decays with third-generation leptons (the τ neutrinos) in the final state. Last but not least, using a representative class of simplified models describing the observed LFU effects, we have analysed the implications of the flavour-conserving, non-universal, quark-lepton contact interactions on $pp \rightarrow \ell^+ \ell^-$ processes at the LHC [21].

- *UV completions.*

A significant step forward has been made on the attempt to find motivated ultraviolet (UV) completions for the simplified models addressing these anomalies. In Ref. [22] the first full-fledged UV complete and calculable gauge model which incorporates the vector lepton-quark as leading mediator for the anomalies has been identified. The model is based on the gauge group $SU(4) \times SU(3) \times SU(2) \times U(1)$, which is assumed to be spontaneously broken to the SM around the TeV scale. A more ambitious attempt has been presented in Ref. [23], with a renormalizable model able to explain the SM flavor hierarchies while, at the same time, accommodating the recent experimental hints of LFU violations in B decays. The latter solution, which can be viewed as a non-trivial extension toward higher energies of the work in Ref. [22], is based on a three-site Pati-Salam gauge group, whose breaking chain down to the SM is illustrated in Figure 2.4. The model is consistent with low- and

high-energy bounds and predicts a rich spectrum of new states at the TeV scale that could be probed in the near future by the high- p_T experiments at the LHC.

- [19] D. Buttazzo, A. Greljo, G. Isidori, and D. Marzocca, *B-physics anomalies: a guide to combined explanations*, JHEP **11** (2017) 044, [arXiv:1706.0780].
- [20] M. Bordone, D. Buttazzo, G. Isidori, and J. Monnard, *Probing Lepton Flavour Universality with $K \rightarrow \pi\nu\bar{\nu}$ decays*, Eur. Phys. J. **C77** (2017), no. 9 618, [arXiv:1705.1072].
- [21] A. Greljo and D. Marzocca, *High- p_T dilepton tails and flavor physics*, Eur. Phys. J. **C77** (2017), no. 8 548, [arXiv:1704.0901].
- [22] L. Di Luzio, A. Greljo, and M. Nardecchia, *Gauge leptoquark as the origin of B-physics anomalies*, Phys. Rev. **D96** (2017), no. 11 115011, [arXiv:1708.0845].
- [23] M. Bordone, C. Cornella, J. Fuentes-Martin, and G. Isidori, *A three-site gauge model for flavor hierarchies and flavor anomalies*, Phys. Lett. **B779** (2018) 317-323, [arXiv:1712.0136].

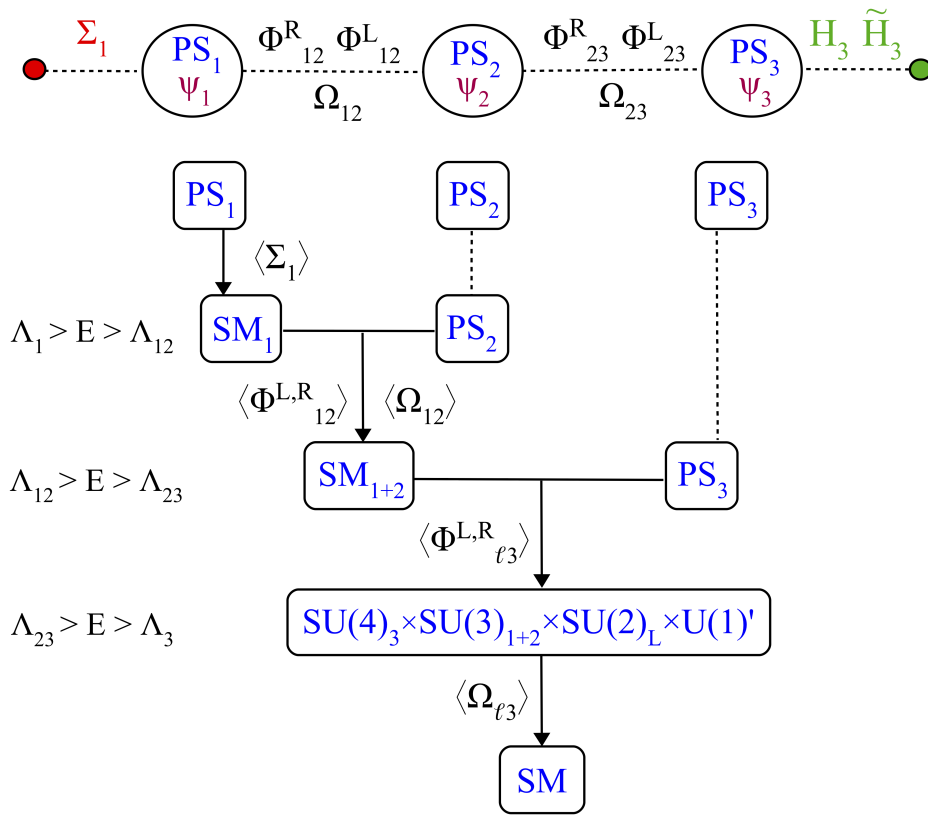


FIG. 2.4 – Symmetry breaking sequence for the three-site Pati-Salam model presented in Ref. [23].